THE JOURNAL OF PHYSICAL CHEMISTRY C

Article

Cite This: J. Phys. Chem. C 2020, 124, 906−912

pubs.acs.org/JPCC

Superconductivity in Sodium Potassium Alloy Doped 2,2′-Bipyridine from Near-Room-Temperature Synthesis

HPSTAR 1089-2020

Di Peng,[†,‡,¶] Ren-Shu Wang,[¶,§] and Xiao-Jia Chen*,[¶]

[†]Key Laboratory of Materials Physics, Institute of Solid State Physics, Chinese Academy of Sciences, Hefei 230031, China

[‡]University of Science and Technology of China, Hefei 230026, China

[¶]Center for High Pressure Science and Technology Advanced Research, Shanghai 201203, China

[§]School of Materials Science and Engineering, Hubei University, Wuhan 430062, China

ABSTRACT: Organic materials especially those with π-electrons have attracted widespread attention because they are promising candidates to exhibit high temperature or even room temperature superconductivity. 2,2′-Bipyridine as a basic raw material is a simple molecule that only contains C, N, and H atoms, and is widely used in metal chelating ligands due to its ease of functionalization and robust redox stability. By doping sodium potassium alloy into 2,2′-bipyridine at approximately room temperature, we successfully detected superconductivity with a critical temperature around 7 K through both the dc and ac magnetic measurements together with the zero resistance state by resistance measurements. Furthermore, the superconducting parameters such as the critical fields, London penetration depth, and Ginzburg−Landau coherence length of the 7 K superconducting phase have been obtained. This finding not only broadens the applications of 2,2′-bipyridine, but also opens an encouraging window for the search of superconductors in photoelectric materials such as pyridine compounds and their derivatives.

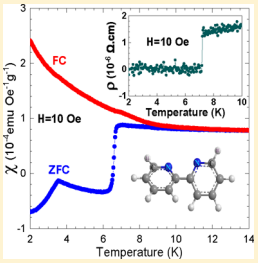

INTRODUCTION

Organic materials, the basis material for all living organisms, are always composed of carbon, hydrogen, nitrogen, etc. Organic materials are of great importance not only for scientific research, looking for high-temperature superconductivity, but also for usual life, since organic materials are both energy-efficient and sustainable. In most cases, organic materials are insulators; however, there have been extensive and intensive efforts in physics and materials science to make them conductive, even superconducting by applying pressure or doping atoms. For instance, the first organic superconductor $(TMTSF)_2PF_6$ was discovered to exhibit superconductivity with a critical temperature (T_c) of 0.9 K at the pressure of 1.2 GPa.[1,2] Later, many cases of introducing charge into π-electron networks in organic superconductors with a Meissner effect were found, such as the alkali metals doped picene,[3] phenanthrene,[4] and 1,2:8,9-dibenzopentacene.[5] However, most of them lacked pivotal zero resistance measurements because of the high doping reaction temperature required that led to the decomposition of organic matter and formation of a nonhomogeneous phase.[6,7] To avoid this tendency, a design principle for a low-temperature synthetic reaction process is indispensable.

Recently, *p*-terphenyl ($C_{18}H_{14}$), which contains three benzene rings connected by C−C bonds, draws much attention due to the discovery of high temperature superconductivity with critical temperatures of 7.2 K,[8] 43 K,[9] and 123 K.[10] The superconducting phase was also observed in potassium-doped biphenyl,[11] *p*-quaterphenyl,[12] and *p*-quinquephenyl.[13] The discovery of superconductivity in potassium-doped *p*-oligophenyls prompts us to ponder whether the π-electrons play a major role in superconductivity due to all the superconducting phases containing π-electrons. Simultaneously, the Meissner effect was also observed in potassium-doped 2,2′-bipyridine.[14] Thus, exploring the superconductivity of alkali-metal-doped 2,2′-bipyridine in near room temperature synthesis is worthy of further exploration.

2,2′-Bipyridine as a neutral ligand has been extensively used in metal chelating ligands due to its ease of functionalization and robust redox stability.[15] The nitrogen atoms in 2,2′-bipyridine can promote energy transfer with the alkali metal, and the steric hindrance of 2,2′-bipyridine with alkali metal coordination is small. Thus, it forms stable charged metal-2,2′-bipyridine complexes with metal cations. Therefore, 2,2′-bipyridine and its derivatives are widely applied in optoelectronics,[16] photonics,[16,17] luminescent devices,[18,19] precursors for helical assembly,[20] and chiral molecular recognition.[21,22] They can form a more stable coordination bond with the alkali metals, which will greatly increase the electron mobility in the charge-transfer complex of alkali metal and 2,2′-bipyridine. If we find a suitable method for doping the alkali metal into 2,2′-bipyridine, the conductivity of the alkali metal doped 2,2′-bipyridine can be greatly improved, and superconductivity may take place. If a superconducting phase can be found in alkali metal doped 2,2′-bipyridine at near room temperature synthesis, it will greatly expand the applications of 2,2′-bipyridine and provide a new avenue for the synthesis of organic superconductors.

Received: October 8, 2019
Revised: December 2, 2019
Published: December 4, 2019

ACS Publications © 2019 American Chemical Society

DOI: 10.1021/acs.jpcc.9b09459
J. Phys. Chem. C 2020, 124, 906−912

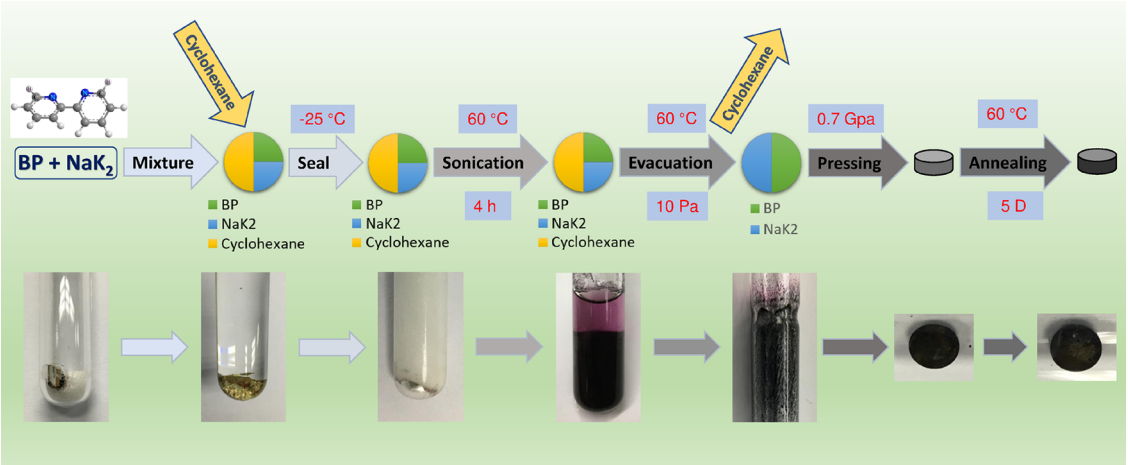

Figure 1. Experimental process diagram of sodium potassium alloy doped 2,2′-bipyridine.

In this paper, we synthesized a uniform sodium potassium alloy doped 2,2′-bipyridine by a liquid−liquid insertion protocol at near room temperature. The near room temperature synthesis avoided the break of the C−H δ-bonds of organic materials at high synthesized temperatures.[23] When the activity of sodium potassium alloy reduced with temperature, the intercalation process dominated the competition between intercalation and molecular decomposition.[6] We report a development method for doping alkali metals into organic materials and forming a homogeneous phase together with the experimental discoveries of superconductivity in sodium potassium alloy doped 2,2′-bipyridine. Meanwhile, this is the first time that superconductivity has been found in doping alkali metal into organic materials at near room temperature, and this low temperature synthetic reaction process is of great significance for doping other alkali metals into organic materials. This discovery is also quite encouraging toward the search of new superconductors in photoelectric materials such as pyridine compounds and their derivatives.

■ METHODS

Material Synthesis. The experimental procedure for doping 2,2′-bipyridine with sodium potassium alloy is shown in Figure 1. High-purity potassium (99%), sodium sticks (99%, coated in film of protective hydrocarbon oil), and 2,2′-bipyridine (99+%) were purchased from Alfa Aesar. Potassium metal was cut into pieces and mixed with small sodium blocks in a molar ratio 2:1. The sodium potassium alloy was then added to a quartz tube. 2,2′-Bipyridine was added to the quartz tube in a molar ratio of 3:2 with sodium−potassium alloy. Cyclohexane as a cosolvent was put into the quartz tube in a molar ratio that is more than 20 times that of 2,2′-bipyridine, and we can see from Figure 1 that almost all of the 2,2′-bipyridine was dissolved in the cyclohexane. All of these operations were done in the glovebox which was filled with argon (O_2 less than 0.1 ppm, H_2O less than 0.1 ppm) to avoid oxidation of sodium and potassium. The mixture in the quartz tube was sealed under vacuum (less than 5×10^{0}Pa) in a solid state at a temperature of approximately minus 25 °C. Then the quartz tube was put into ultrasonic processor where the temperature was set up to 60 °C. At this temperature, the sodium−potassium alloy was gradually dispersed into small particles under the action of severe ultrasonic waves. After about 4 h of ultrasonic processing, the mixture in the quartz tube turned to a uniform black suspension liquid. After the black suspension liquid was vacuumed at a temperature of approximately 60 °C, the cosolvent cyclohexane was removed and we obtained a black powder sample. The black powder was pressed into a cylinder with a pressure of approximately 0.7 GPa through a mold with a diameter of 6 mm. The cylindrical sample was put into a quartz tube and sealed under high vacuum (less than 5×10^{-3}Pa). Then, the quartz tube was heated up to 60 °C for 5 days to obtain a more uniform sample phase. The final products after heat treating were black (as shown in the bottom right of Figure 1) and also sensitive to air.

Material Characterization. We measured the zero-field-cooling (ZFC) and field-cooling (FC) modes under 20 Oe by a SQUID magnetometer (Quantum Design MPMS3) in the temperature range of 1.8−300 K, and the magnetic field was applied to the axis of pellets in the measurements. The four copper electrodes were prearranged in a spiral shape and were placed in the powder sample, and then the electrodes and the sample were pressed together into a cylindrical shape in a mold by the pressure of about 1 GPa. The resistance measurement was made by PPMS (Quantum Design). One end of each copper wire was connected to the cylindrical sample and the other end was connected to the PUCK (as shown in the top right of Figure 5). To compare the vibration modes between pristine and sodium potassium alloy doped 2,2′-bipyridine, the Raman scattering spectra were collected at room temperature at a wavelength of 488 nm and power at 2 mW.

■ RESULTS AND DISCUSSION

Figure 2 shows the temperature dependence of magnetic susceptibility measured in the zero-field-cooling (ZFC) and field-cooling (FC) runs for $(NaK_2)_x$2,2-bipyridine under different magnetic fields. The magnetic susceptibility for $(NaK_2)_x$2,2-bipyridine near the step transition temperature is shown, which clearly presents the superconducting transition at 6.7 and 3.5 K. As can be seen from the illustration in Figure 2, the χ value of the 6.7 K superconducting phase decreases rapidly, and the transition width between T_c^{onset} and T_c^{end} is less than 0.4 K. However, the superconducting phase of 3.5 K drops slowly and has a wide transition width. By analyzing the temperature dependence of magnetic susceptibility in Figure 2, the obvious Meissner effect can be observed. The Meissner effect is one of the fundamental properties for defining superconductivity. The field-cooling measurements show a

DOI: 10.1021/acs.jpcc.9b09459
J. Phys. Chem. C 2020, 124, 906−912

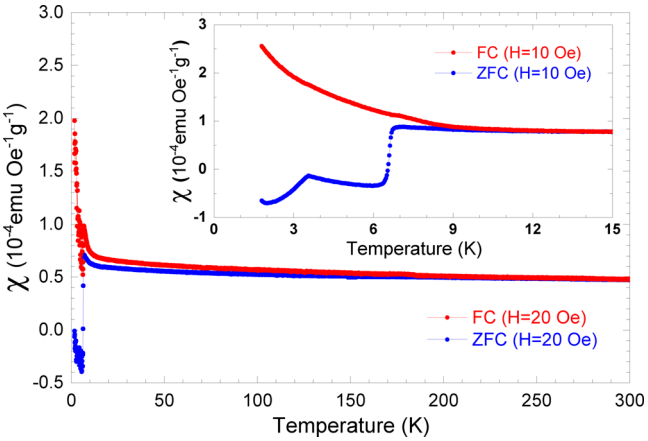

Figure 2. Temperature dependence of magnetic susceptibility measured in the zero-field-cooling (ZFC) and field-cooling (FC) runs for $(NaK_2)_x$2,2′-bipyridine at the magnetic fields of 20 Oe. The inset shows the temperature dependence of magnetic susceptibility in ZFC and FC runs for $(NaK_2)_x$2,2′-bipyridine from 1.8 to 15 K at the magnetic fields of 10 Oe.

weak flux expulsion by contrast with the zero-field-cooling results, suggesting the existence of pinning. In these systems, the energy dissipation is caused by the motion of vortices. The motion of vortices can be reduced or eliminated by providing pinning centers to "pin" the vortex lattice.[24] Typically these are just impurities, or naturally occurring crystal defects such as grain boundaries and dislocations. When the field exceeds the upper critical field, there is a weak paramagnetic signal. However, the origins of this paramagnetic moment remain unsettled.[25] The reason why there is a weak upturn at low temperature is that the products contain a positive paramagnetic background and the shielding fraction is also small. Supposing that the density δ of this sample is about 3 g/cm^3, we get the shielding fraction $4\pi\chi\delta$ = 0.46% from Figure 2. The shielding fraction of the superconducting content is not very high because of the presence of impurities.

Figure 3 presents the temperature dependence of imaginary part and real part of the alternating current (ac) magnetic

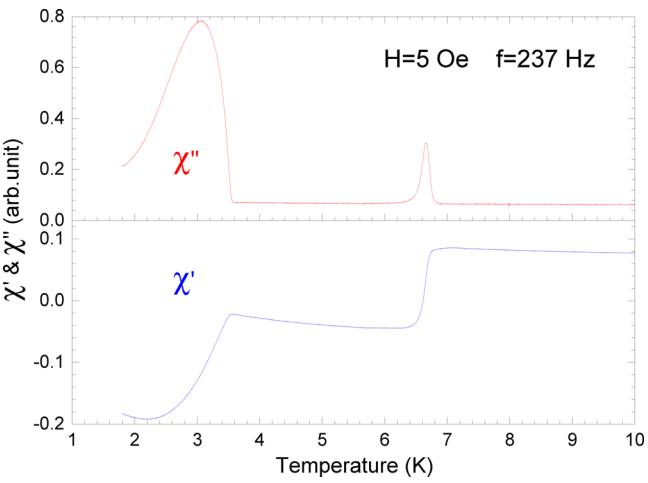

Figure 3. Temperature dependence of the imaginary part and real part of the ac magnetic susceptibility of $(NaK_2)_x$2,2′-bipyridine. The frequency and amplitude of applied field are 237 Hz and 5 Oe, respectively.

susceptibility of $(NaK_2)_x$2,2′-bipyridine at 5 Oe and a frequency of 237 Hz. The susceptibility measurements of ac as a powerful signature of the occurrence of superconductivity in samples are widely used in magnetic studies of superconductors because they are nondestructive to the samples. The complex susceptibility $\chi = \chi' + i\chi''$ has a little different meaning from direct current (dc) magnetic susceptibility. The real part χ' corresponds to the differential quantity dM/dH and is approximately equal to the ZFC magnetic susceptibility in the dc measurement.[26] Therefore, it is also a method of measuring the shielding response of a superconductor. The imaginary part χ'' corresponds to the energy dissipation in a material.[27,28] From the complex χ, we can deduct some parameters of superconductivity, such as T_c, lower and upper critical fields, London and Campbell penetration depths, the pining potential, irreversibility line, and critical current density, etc.[29] The imaginary part χ'' arises from the formation of the weakly linked superconducting vortex current. Thus, χ'' can be considered as a testification of the zero resistance because it is a superconducting signal of this material. The real part of Figure 2 shows two step-like transitions occurring at the temperature of 3.5 and 6.7 K, which have almost the same characteristics as the T_c value already determined from dc magnetic susceptibility at Figure 2. Meanwhile, two positive peaks appear in the imaginary part at the temperature of 3.5 and 6.7 K, indicating that the ac field penetrates the sample. Hence, from the results of the ac measurements, it can be seen that two superconducting phases in our sample appear at 3.5 and 6.7 K, respectively. The peak of 6.7 K appears in the imaginary part implying zero resistivity in the superconducting state, which is basically consistent with the results of the following resistance measurements.

The obtained superconductivity in sodium potassium alloy doped 2,2′-bipyridine is further supported by the evolution of the $\chi-T$ curves with the applied magnetic fields (Figure 4).

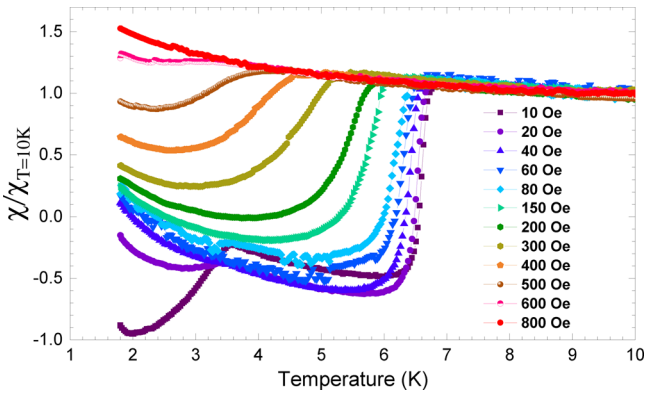

Figure 4. Temperature dependence of the magnetic susceptibility of $(NaK_2)_x$2,2′-bipyridine measured at various magnetic fields up to 800 Oe in the zero-field-cooling (ZFC) run.

The diamagnetic signal disappears gradually with the increasing magnetic field since the superconducting phase is suppressed by the applied magnetic field. In the magnetic field above 60 Oe, the diamagnetic signal of the 3.5 K superconducting phase is hardly visible, but the diamagnetic signal of the 6.7 K superconducting phase does not disappear until 800 Oe or more. The $\chi-T$ curves at various magnetic fields demonstrate that the obtained superconductivity is intrinsic to $(NaK_2)_x$2,2′-bipyridine. The diamagnetic signal of the 3.5 K

DOI: 10.1021/acs.jpcc.9b09459
J. Phys. Chem. C 2020, 124, 906−912

superconducting phase is quickly reduced and almost disappears at 100 Oe due to the existence of a dominant paramagnetic phase, which further suggests that the diamagnetic volume shielding fraction is too small and there is a positive paramagnetic background at low temperatures. Obviously, as the magnetic field is increased, the paramagnetic signal increases at a rate greater than that of the diamagnetic signal.

Figure 5 plots the resistivity versus temperature curves from 2 to 300 K at zero field in the two modes of warming and

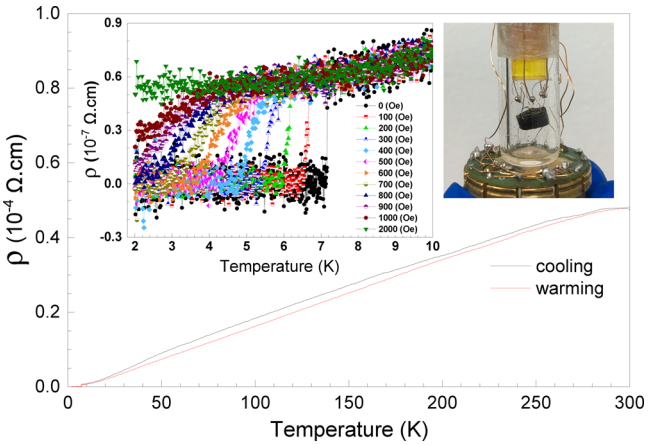

Figure 5. Temperature dependence of the resistance of $(NaK_2)_x$2,2′-bipyridine from 2 to 300 K. Inset shows the resistivity versus temperature curves measurements under different magnetic fields.

cooling, and the inset shows the resistivity versus temperature curves from 2 to 10 K with varying magnetic fields. Since the shielding fraction volume of this sample is too small, the resistance measurements are very difficult. We built a completely sealed environment to measure the resistance of $(NaK_2)_x$2,2′-bipyridine by the four-probe method (as shown in the inset of Figure 5). The resistance exhibits obvious metal properties at the normal state, but because the sample was pressed into a cylindrical shape in a mold with a pressure of about 1 GPa, the metallic feature possibly comes from the sodium potassium alloy. From the figure we can see that the resistance exhibits a drastic drop at around 7.2 K. This phenomenon indicates a clear superconducting transition. However, since the measured value is close to the measurement limit of the instrument, the random background noise of the resistance data is strong near the superconducting transition temperature. From the figure we can see that the resistance drops sharply around 7.1 K in zero-field, which precisely indicates the existence of a superconducting transition. The T_c of 7.1 K is slightly higher than the dc and ac susceptibility measurements probably due to the sample being pressurized to 1 GPa before the resistance measurement, but the effect of pressure on the superconducting transition temperature requires further studies. The inset of Figure 5 shows the resistivity as a function of temperature in the dc magnetic field from 0 to 2000 Oe. It can be clearly seen from the inset that the superconductivity is gradually suppressed as the magnetic field increases, and the superconducting transition width exhibits a significant broadening at high fields. We measured a zero-resistance effect in samples with such small shielding fraction volume, which illustrates the effectiveness of the method of measuring resistance. We can measure the zero-resistance effect of this sample perhaps because of the intercalation of sodium potassium alloy into 2,2′-bipyridine and the formation of a charge-transfer complex inducing an appearance of 1D electron percolating networks that regulate the conductivity[30] and form a superconducting network.

Figure 6 shows the magnetization hysteresis loop with magnetic fields up to 800 Oe measured at various temperatures

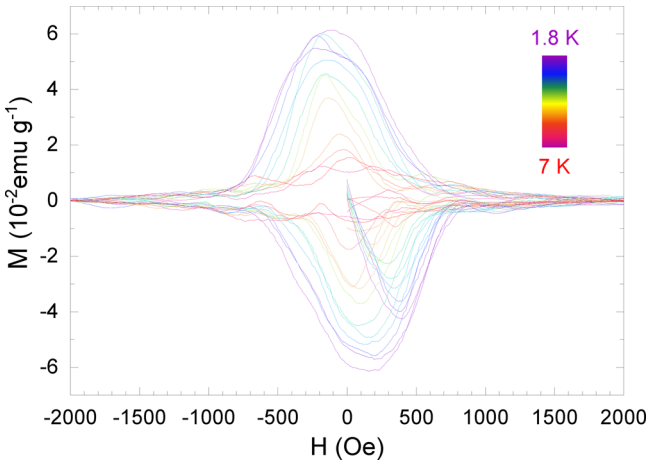

Figure 6. Magnetization hysteresis loop with scanning magnetic field up to 800 Oe measured at various temperatures in the superconducting state after the subtraction of the magnetic background at 7.5 K.

between 1.8 and 7 K in the superconducting state after the subtraction of the magnetic background at 7.5 K. The paramagnetic background signal has been deducted in order to eliminate the influence of magnetic impurities. The hysteresis loop along the two opposite magnetic field directions provides evidence that this superconducting phase is a typical type-ii superconductor. The asymmetry along the vertical $H = 0$ axis provides evidence for the wide-band susceptibilities.[29] The diamond-like shape expands from the inner to the outer with the decrease of temperature, yielding a higher upper critical field in the horizontal axis for a lower temperature.

Figure 7 shows the temperature dependence of the lower critical field $H_{c1}(T)$ and the upper critical field $H_{c2}(T)$. The inset at the left bottom shows how H_{c1} is determined by a given temperature based on the deviation of the linear behavior at higher field. We use the empirical law $H_{c1}(T)/H_{c1}(0) = 1 - (T/T_c)^2$ to calculate the lower critical field at zero temperature $H_{c1}(0)$. Then the zero-temperature extrapolated value of $H_{c1}(0)$ is 136 ± 2 Oe. The upper critical field H_{c2} is defined by T_c at an applied field, and the T_c is determined by the linear extrapolation intercept of the transition section below and above, as shown in the right upper. H_{c2} can be determined from the resistivity versus temperature curves measured at various magnetic fields and the obtained $H_{c2}(T)$ as a function of temperature is shown in Figure 7. Using the Werthamer−Helfand−Hohenberg formula,[31] the zero-temperature $H_{c2}(0)$ = 1555 ± 11 Oe is obtained. From $H_{c2}(0)$ and $H_{c1}(0)$, using the expressions $H_{c2}(0) = \phi_0/2\pi\xi^2_{GL}$ and $H_{c1}(0) = (\phi_0/4\pi\lambda^2_L)(\ln\lambda_L/\xi_{GL})$[32] with the flux quantum $\Phi_0 = 2.0678 \times 10^{-15}$ Wb, we evaluate the zero-temperature superconducting London penetration depth λ_L and Ginzburg−Landau coherence length ξ_{GL}. Substituting the obtained $H_{c2}(0)$ and $H_{c1}(0)$,

DOI: 10.1021/acs.jpcc.9b09459
J. Phys. Chem. C 2020, 124, 906−912

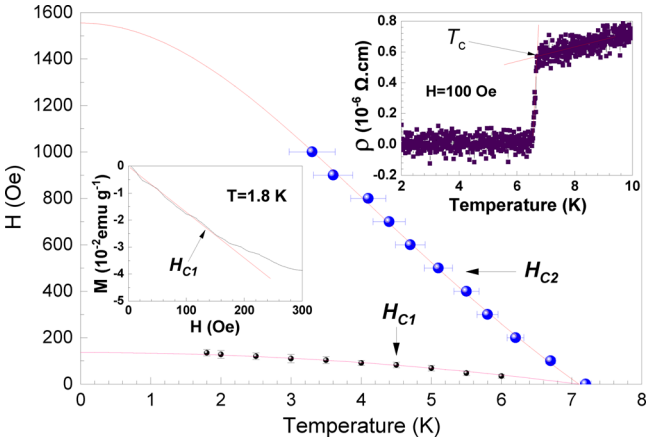

Figure 7. Temperature dependence of the lower critical field $H_{c1}(T)$. The error bars represent estimated uncertainty in determining H_{c1}. The solid line represents the empirical law $H_{c1}(T)/H_{c1}(0) = 1 - (T/T_c)^2$. The inset at the bottom left shows the determination of H_{c1} and the magnetic field dependence of magnetization at the temperature of 1.8 K. The temperature dependence of the upper critical field $H_{c2}(T)$. The error bars represent the uncertainty in the rounding of the transition. The line is the fitting to the Werthamer−Helfand−Hohenberg theory.[31] The inset at the upper right shows an example used to definite T_c by the temperature dependence of magnetization at the field of 10 Oe.

we obtain ξ_{GL} = 46 ± 1 nm and λ_L = 78 ± 2 nm for this superconducting phase. As discussed by Mitsuhashi et al.,[3] the London penetration depth (λ_L = 78 ± 2 nm) is larger than the crystal lattice size, resulting in the small shielding fraction of the powder sample. Thus, the Ginzburg−Landau parameter $\kappa = \lambda_L/\xi_{GL} = 1.69 > 1/\sqrt{2}$ is obtained, implying that the $(NaK_2)_x$2,2′-bipyridine is a type-ii superconductor. For type-ii materials perfect diamagnetism occurs only below H_{c1}, while the superconducting phase between H_{c1} and H_{c2} is the Abrikosov or mixed state.

Raman spectroscopy is a powerful phase-sensitive tool to identify the molecular dynamics process and structural transformation of organic materials.[33] The Raman spectra of the pristine and sodium potassium-alloy-doped 2,2′-bipyridine, obtained by using a laser wavelength of 488 nm at room temperature, are displayed in Figure 8, respectively. It is shown that the high frequency pure C−H stretching vibrations lying around 3078 cm^{-1} almost disappear after doping. When 2,2′-bipyridine is doped by a sodium potassium alloy, a new ring stretching mode is generated at 1497 cm^{-1}, accompanied by the disappearance of the ring stretching mode at 1591 cm^{-1} and the *trans* conformer band at 1449 cm^{-1}.[34] The ring stretching mode at 1239 cm^{-1} and the C−H in-plane deformation at 1304 cm^{-1} show blue shift to the position of 1263 and 1346 cm^{-1}, respectively, suggesting an increase of π-electrons polarization in 2,2′-bipyridine after sodium and potassium alloy doping. The ring stretching mode at 1574 cm^{-1} and the C−H in-plane deformation at 1484 cm^{-1} exhibit a red-shift to a small wide peak at 1565 cm^{-1} and the position of 1467 cm^{-1}, respectively.[34,35] The ring breathing mode at 996 cm^{-1} also exhibits a red-shift after doping to the polaron bands at 977 cm^{-1}.[36,37] Simultaneously, the three vibrations at 996 cm^{-1}, 1346 cm^{-1}, and 1467 cm^{-1} also suggest the formation of bipolarons.[36,38] All of the above red shifts were attributed to the softening of Raman modes by the transferred electrons from the sodium potassium alloy to 2,2′-bipyridine.[39−41] There are 17 and 19 cm^{-1} downshifts for the C−H in-plane deformation at 1484 and 1046 cm^{-1} together with 19 cm^{-1} downshifts for the ring breathing mode at 996 cm^{-1} in sodium potassium alloy doped 2,2′-bipyridine. The red shift of these modes indicates that approximately three electrons have been transferred from the sodium potassium alloy to 2,2′-bipyridine, and this is consistent with the 6 cm^{-1} per electron and 7 cm^{-1} per electron red shifts observed in superconducting A_3phenanthrene (A = K, Rb)[4] and A_3C_{60} (A = K, Rb).[44] The red shifts of the Raman spectrum indicate the presence of a charge transfer complex in the sodium potassium alloy doped 2,2′-bipyridine together with the formation of polaron and bipolarons, which greatly improves the conductivity of the sample.[30,42,43] The increase in resistivity can also be seen from the resistivity versus temperature curves in Figure 5 that the sample is close to the metallic state. The nitrogen element in the 2,2′-bipyridine molecule has the largest electronegativity and the strongest electron attracting ability. Thus, 2,2′-bipyridine can form a more stable coordination bond with sodium and potassium atoms, which will greatly increase the electron mobility in the charge-transfer complex of doped samples. This is consistent with that observed in the resistivity versus temperature curves and the red shifts of Raman spectra between the pristine and doped sample. So we propose that the doped sodium and potassium atoms are at the closest position to the nitrogen atom.

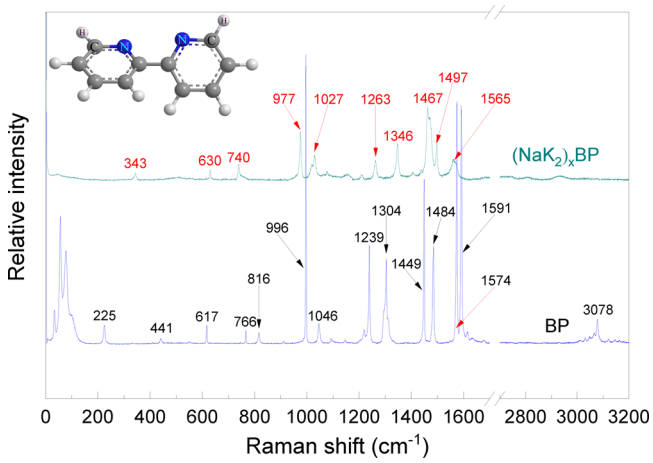

Figure 8. Raman spectra of pristine 2,2′-bipyridine and $(NaK_2)_x$2,2′-bipyridine collected at room temperature. Upper left presents the molecular structure of 2,2′-bipyridine. The sticks in the main panel give the peak positions of the pristine and doped samples.

■ CONCLUSIONS

We have used an ultrasonic-assisted solvent method to disperse the sodium potassium alloy, so that sodium and potassium atoms can be doped into the 2,2′-bipyridine at low temperature and avoid the decomposition of 2,2′-bipyridine in high-temperature synthesis. Simultaneously, this method can be used for doping alkali metal atoms into other organic materials at low temperatures.

We have successfully observed a superconducting phase with the critical temperature around 7 K through both the dc and ac magnetic measurements together with the zero resistance state by resistance measurements. The upper critical field and lower critical field were calculated from the $\chi-T$ curve with the applied magnetic fields and the resistivity versus temperature curves measured at various magnetic fields, respectively. Some

DOI: 10.1021/acs.jpcc.9b09459
J. Phys. Chem. C 2020, 124, 906−912

of the superconducting parameters have been obtained, and the Ginzburg−Landau parameter κ provides evidence for type-ii superconductors.

The discovery of superconductivity in sodium potassium alloy doped 2,2′-bipyridine provides unambiguous evidence that the π-electrons play an important role in boosting superconductivity. As compared with polycyclic aromatic hydrocarbons and poly p-phenylene(PPP), 2,2′-bipyridine is more likely to form a stable coordination bond with an alkali metal due to the nitrogen atoms. Therefore, it is easy to form a stable high conductivity charge transfer complex and finally achieve superconductivity.

The present finding of the Meissner effect and zero resistance state in sodium potassium alloy doped 2,2′-bipyridine is extremely encouraging in the search of a new superconducting phase in pyridine compounds and their derivatives. This finding expands the applications of 2,2′-bipyridine and provides a new avenue for searching new superconductors in photoelectric materials. Our ongoing work focuses on further improving the diamagnetic volume shielding fraction through a suitable pressurized heat treatment and the development of a synthetic method.

■ AUTHOR INFORMATION

Corresponding Author

*E-mail: xjchen@hpstar.ac.cn. Phone: +86 (0)21 80177044. Fax: +86 (0)21 80177064.

ORCID

Di Peng: 0000-0002-4235-6385
Xiao-Jia Chen: 0000-0003-3921-9424

Notes

The authors declare no competing financial interest.

■ ACKNOWLEDGMENTS

This work was supported by the National Key R&D Program of China (Grant No. 2018YFA0305900).

■ REFERENCES

(1) Jérome, D.; Mazaud, A.; Ribault, M.; Bechgaard, K. Superconductivity in a synthetic organic conductor $(TMTSF)_2PF_6$. *J. Phys., Lett.* **1980**, *41*, 95−98.

(2) Vuletić, T.; Auban-Senzier, P.; Pasquier, C.; Tomić, S.; Jérome, D.; Héritier, M.; Bechgaard, K. Coexistence of superconductivity and spin density wave orderings in the organic superconductor $(TMTSF)_2PF_6$. *Eur. Phys. J. B* **2002**, *25*, 319−331.

(3) Mitsuhashi, R.; Suzuki, Y.; Yamanari, Y.; Mitamura, H.; Kambe, T.; Ikeda, N.; Okamoto, H.; Fujiwara, A.; Yamaji, M.; Kawasaki, N.; et al. Superconductivity in alkali-metal-doped picene. *Nature* **2010**, *464*, 76−79.

(4) Wang, X. F.; Liu, R. H.; Gui, Z.; Xie, Y. L.; Yan, Y. J.; Ying, J. J.; Luo, X. G.; Chen, X. H. Superconductivity at 5 K in alkali-metal-doped phenanthrene. *Nat. Commun.* **2011**, *2*, 507.

(5) Xue, M.; Cao, T.; Wang, D.; Wu, Y.; Yang, H.; Dong, X.; He, J.; Li, F.; Chen, G. F. Superconductivity above 30 K in alkali-metal-doped hydrocarbon. *Sci. Rep.* **2012**, *2*, 389.

(6) Zhang, J.; Whitehead, G. F. S.; Manning, T. D.; Stewart, D.; Hiley, C. I.; Pitcher, M. J.; Jansat, S.; Prassides, K.; Rosseinsky, M. J. The reactivity of solid rubrene with potassium: competition between intercalation and molecular decomposition. *J. Am. Chem. Soc.* **2018**, *140*, 18162−18172.

(7) Valenti, R.; Winter, S. M. Polycyclic aromatic hydrocarbons: Synthesis successes. *Nat. Chem.* **2017**, *9*, 608−609.

(8) Wang, R. S.; Gao, Y.; Huang, Z. B.; Chen, X. J. Superconductivity in p-terphenyl, arXiv:1703.05803.https://arxiv.org/abs/1703.05803 (submitted Mar 16, 2017).

(9) Wang, R. S.; Gao, Y.; Huang, Z. B.; Chen, X. J. Superconductivity at 43 K in a single C-C bond linked terphenyl, arXiv:1703.05804. https://arxiv.org/abs/1703.05804 (submitted Mar 16, 2017).

(10) Wang, R. S.; Gao, Y.; Huang, Z. B.; Chen, X. J. Superconductivity above 120 K in a chain link molecule, arXiv:1703.06641. https://arxiv.org/abs/1703.06641 (submitted Mar 20, 2017).

(11) Zhong, G. H.; Yang, D. Y.; Zhang, K.; Wang, R. S.; Zhang, C.; Lin, H. Q.; Chen, X. J. Superconductivity and phase stability of potassium-doped biphenyl. *Phys. Chem. Chem. Phys.* **2018**, *20*, 25217−25223.

(12) Yan, J. F.; Zhong, G. H.; Wang, R. S.; Zhang, K.; Lin, H. Q.; Chen, X. Superconductivity and Phase Stability of Potassium-Intercalated p-Quaterphenyl. *J. Phys. Chem. Lett.* **2019**, *10*, 40−47.

(13) Huang, G.; Zhong, G. H.; Wang, R. S.; Han, J. X.; Lin, H. Q.; Chen, X. J. Superconductivity and phase stability of potassium-doped p-quinquephenyl. *Carbon* **2019**, *143*, 837−843.

(14) Zhang, K.; Wang, R. S.; Qin, A. J.; Chen, X. J. Superconductivity in potassium-doped 2,2′-bipyridine, arXiv:1801.06320. https://arxiv.org/abs/1801.06320 (submitted Jan 24, 2018).

(15) Kaes, C.; Katz, A.; Hosseini, M. W. Bipyridine: the most widely used ligand. A review of molecules comprising at least two 2,2′-bipyridine units. *Chem. Rev.* **2000**, *100*, 3553−3590.

(16) Kalyanasundaram, K.; Grätzel, M. Applications of functionalized transition metal complexes in photonic and optoelectronic devices. *Coord. Chem. Rev.* **1998**, *177*, 347−414.

(17) Baxter, S. M.; Jones, W. E.; Danielson, E.; Worl, L.; Strouse, G.; Younathan, J.; Meyer, T. J. Photoinduced electron and energy transfer in soluble polymers. *Coord. Chem. Rev.* **1991**, *111*, 47−71.

(18) Ward, M. D.; White, C. M.; Barigelletti, F.; Armaroli, N.; Calogero, G.; Flamigni, L. Assemblies of luminescent ruthenium(II)- and osmium(II)-polypyridyl complexes based on hydrogen bonding. *Coord. Chem. Rev.* **1998**, *171*, 481−488.

(19) Balzani, V.; Juris, A.; Venturi, M.; Campagna, S.; Serroni, S. Luminescent and redox-active polynuclear transition metal complexes. *Chem. Rev.* **1996**, *96*, 759−833.

(20) Piguet, C.; Bernardinelli, G.; Hopfgartner, G. Helicates as versatile supramolecular complexes. *Chem. Rev.* **1997**, *97*, 2005−2062.

(21) Knof, U.; Zelewsky, A. V. Predetermined chirality at metal centers. *Angew. Chem., Int. Ed.* **1999**, *38*, 303−322.

(22) Belser, P.; Bernhard, S.; Jandrasics, E.; Zelewsky, A. V.; Cola, L. D.; Balzani, V. Synthesis and photophysical properties of chiral, binuclear metal complexes. *Coord. Chem. Rev.* **1997**, *159*, 11−18.

(23) Romero, F. D.; Pitcher, M. J.; Hiley, C. I.; Whitehead, G. F. S.; Kar, S.; Ganin, A. Y.; Antypov, D.; Collins, C.; Dyer, M. S.; Klupp, G.; et al. Redox-controlled potassium intercalation into two polyaromatic hydrocarbon solids. *Nat. Chem.* **2017**, *9*, 644−652.

(24) Dmitriev, A. V. James F. Annett. Superconductivity superfluids and condensates, Oxford University Press (Oxford master series in condensed matter physics): 2004; 186 pages (approximate price $40). *Mater. Res. Bull.* **2005**, *40*, 1233−1234.

(25) Weller, T. E.; Ellerby, M.; Saxena, S. S.; Smith, R. P.; Skipper, N. T. Superconductivity in the intercalated graphite compounds C_6Yb and C_6Ca. *Nat. Phys.* **2005**, *1*, 39−41.

(26) Lee, M. W.; Tai, M. F.; Luo, S. C.; Shi, J. B. Critical current densities in K_3C_{60}/Rb_3C_{60} powders determined from AC/DC susceptibility measurements. *Phys. C* **1995**, *245*, 6−11.

(27) Hafiez, M. A.; Zhang, Y. Y.; Cao, Z. Y.; Duan, C. G.; Karapetrov, G.; Pudalov, V. M.; Vlasenko, V. A.; Sadakov, A. V.; Knyazev, D. A.; Romanova, T. A.; Chareev, D. A.; et al. Superconducting properties of sulfur-doped iron selenide. *Phys. Rev. B: Condens. Matter Mater. Phys.* **2015**, *91*, 165109.

(28) García, J.; Rillo, C.; Lera, F.; Bartolomé, J.; Navarro, R.; Blank, D. H. A.; Flokstra, J. Superconducting weak links in YBa2Cu3O7σ an AC magnetic susceptibility study. *J. Magn. Magn. Mater.* **1987**, *69*, 225−229.

DOI: 10.1021/acs.jpcc.9b09459
J. Phys. Chem. C 2020, 124, 906−912

(29) Gömöry, F. TOPICAL REVIEW: Characterization of high-temperature superconductors by AC susceptibility measurements. *Supercond. Sci. Technol.* **1997**, *10*, 523−542.
(30) Hu, Y.; Zhong, G. H.; Guan, Y. S.; Lee, N. H.; Zhang, Y.; Li, Y.; Mitchell, T.; Armstrong, J. N.; Benedict, J.; Hla, S. W.; et al. Alkali-Metal-Intercalated Percolation Network Regulates Self-Assembled Electronic Aromatic Molecules. *Adv. Mater.* **2019**, *31*, No. e1807178.
(31) Werthamer, N. R.; Helfand, E.; Hohenberg, P. C. Temperature and Purity Dependence of the Superconducting Critical Field, H_{c2}. III. Electron Spin and Spin-Orbit Effects. *Phys. Rev.* **1966**, *147*, 255−263.
(32) Tinkham, M.; Wheatley, J. C. Introduction to Superconductivity. *Phys. Today* **1976**, *29*, 57−57.
(33) Zawada, K.; Bukowska, J. Surface-enhanced Raman spectroscopy and electrochemistry of 2,2′-bipyridine adsorbed at copper electrode. *Electrochim. Acta* **2004**, *49*, 469−476.
(34) Castellà-Ventura, M.; Kassab, E.; Buntinx, G.; Poizat, O. Structure of the anion radical of 2,2′-bipyridine in solution. *Phys. Chem. Chem. Phys.* **2000**, *2*, 4682−4689.
(35) Moissette, A.; Batonneau, Y.; Brémard, C. Conformation and protonation of 2,2′-bipyridine and 4,4′-bipyridine in acidic aqueous media and acidic ZSM-5 zeolites: a Raman scattering study. *J. Am. Chem. Soc.* **2001**, *123*, 12325−12334.
(36) Dubois, M.; Froyer, G.; Louarn, G.; Billaud, D. Raman spectroelectrochemical study of sodium intercalation into poly(*p*-phenylene). *Spectrochim. Acta, Part A* **2003**, *59*, 1849−1856.
(37) Furukawa, Y.; Ohtsuka, H.; Tasumi, M. Raman studies of polarons and bipolarons in sodium-doped poly-p-phenylene. *Synth. Met.* **1993**, *55*, 516−523.
(38) Furukawa, Y.; Ohtsuka, H.; Tasumi, M.; Wataru, I.; Kanbara, T.; Yamamoto, T. Raman Studies of Intact and Sodium Doped ^{13}C-substituted Poly-*p*-phenylene. *J. Raman Spectrosc.* **1993**, *24*, 551−554.
(39) Kubozono, Y.; Mitamura, H.; Lee, X.; He, X.; Yamanari, Y.; Takahashi, Y.; Suzuki, Y.; Kaji, Y.; Eguchi, R.; Akaike, K.; et al. Metal-intercalated aromatic hydrocarbons: a new class of carbon-based superconductors. *Phys. Chem. Chem. Phys.* **2011**, *13*, 16476−16493.
(40) Wang, R. S.; Cheng, J.; Wu, X. L.; Yang, H.; Chen, X. J.; Gao, Y.; Huang, Z. B. Superconductivity at 3.5 K and/or 7.2 K in potassium-doped triphenylbismuth. *J. Chem. Phys.* **2018**, *149*, 144502.
(41) Huang, Q. W.; Zhong, G. H.; Zhang, J.; Zhao, X. M.; Zhang, C.; Lin, H. Q.; Chen, X. J. Constraint on the potassium content for the superconductivity of potassium-intercalated phenanthrene. *J. Chem. Phys.* **2014**, *140*, 114301.
(42) Kambe, T.; He, X.; Takahashi, Y.; Yamanari, Y.; Teranishi, K.; Mitamura, H.; Shibasaki, S.; Tomita, K.; Eguchi, R.; Goto, H.; et al. Synthesis and physical properties of metal-doped picene solids. *Phys. Rev. B: Condens. Matter Mater. Phys.* **2012**, *86*, 214507.
(43) Rao, A. M.; Eklund, P. C.; Bandow, S.; Thess, A.; Smalley, R. E. Evidence for charge transfer in doped carbon nanotube bundles from Raman scattering. *Nature* **1997**, *388*, 257−259.
(44) Zhou, P.; Wang, K.-A.; Wang, Y.; Eklund, P. C.; Dresselhaus, M. S.; Dresselhaus, G.; Jishi, R. A. Raman scattering in C_{60} and alkali-metal-saturated C_{60}. *Phys. Rev. B: Condens. Matter Mater. Phys.* **1992**, *46*, 2595−2605.

DOI: 10.1021/acs.jpcc.9b09459
J. Phys. Chem. C 2020, 124, 906−912